



## Variability regimes of simulated Atlantic MOC

Xiuhua Zhu,<sup>1,2</sup> Klaus Fraedrich,<sup>3</sup> and Richard Blender<sup>3</sup>

Received 26 June 2006; revised 1 August 2006; accepted 26 September 2006; published 4 November 2006.

[1] The spectral variability structure of the meridional overturning circulation (MOC) of the Atlantic Ocean is determined in 500 year simulations with state-of-the-art coupled atmosphere-ocean general circulation models (GFDL and ECHAM5/MPIOM). The power spectra of the monthly stream function are compared with trend-eliminating detrended fluctuation analysis (DFA2). The shapes of the spectra differ substantially between latitudes, depth and the two models with constant (white) behaviour for high frequencies as a single common feature. The most frequent property of the spectra is power-law scaling,  $S(f) \sim f^{-\beta}$ , with nontrivial exponents, mostly  $\beta \approx 1$ , in agreement with  $1/f$  or flicker noise; this is mainly found in the interannual to decadal frequency range ( $1/f$  spectra observed for sea surface temperature fluctuations are explained by a stochastically forced ocean energy balance model with vertical diffusion). For lowest frequencies, some spectra show stationary long term memory, while others reveal spectra increasing with frequency. None of the spectra can be considered uniquely as red noise explained by an ocean integrating a white stochastic atmospheric forcing.  
**Citation:** Zhu, X., K. Fraedrich, and R. Blender (2006), Variability regimes of simulated Atlantic MOC, *Geophys. Res. Lett.*, 33, L21603, doi:10.1029/2006GL027291.

### 1. Introduction

[2] Climate variability is present on many time scales, ranging from seasons to millennia [Huybers and Curry, 2006]. In the northern North Atlantic available instrumental records of sea surface temperature (SST) show low frequency variability (LFV, i.e. increasing power with decreasing frequency) in terms of power-law scaling up to decades [Fraedrich and Blender, 2003] revealing  $1/f$  spectra (flicker noise) in particular regions. The  $1/f$  spectra of SST can be explained by an ocean energy balance model with vertical diffusion forced by stochastic atmospheric surface and advective ocean heat fluxes [Fraedrich et al., 2004]. These advective processes in the North Atlantic, which are related to the dynamics of the subtropical gyre, have also been identified as a source of oscillations [Eden et al., 2002; Eden and Greatbatch, 2003] and LFV [Junge and Fraedrich, 2006].

[3] Defining the MOC as a circulation of mass, heat and salt, its variability is subject to processes which lead to changes of the mass, heat and salt transport, such as surface

buoyancy forcing, wind forcing and internal ocean dynamics. For high frequency (intra-annual and annual) time scales, the spectrum is white. On these time scales, wind forcing dominates the MOC fluctuations [see, e.g., Jayne and Marotzke, 2001], which is related to linear, barotropic dynamics [Willebrand et al., 1980]. In the transitional frequency regime, the scaling behaviour is associated with the ocean's self-adjustment of the density field. The east-west density gradient can be induced by both wind stress and buoyancy forcing [Sturges and Hong, 1995; Delworth and Greatbatch, 2000]. Frankignoul et al. [1997] found that this 'reddening' process is related to the westward propagation of the baroclinic Rossby waves and determined by the wave speed and basin width. In addition, oscillations have been identified in the North Atlantic at periods of about 30 years (compare Delworth and Greatbatch [2000], Eden and Greatbatch [2003], Eden and Jung [2001], Eden and Willebrand [2001]).

[4] The first generation of dynamic ocean models has reproduced LFV, which, however, was not unique for all models. This lead to the conjecture that LFV is possibly due to model deficiencies since the oceanic circulation was assumed to be white on long time scales [von Storch et al., 2000]. Relevant model deficiencies are too coarse resolutions and the parameterisation of the vertical diffusion. However, it was shown that a 10 ky simulation with a first generation AOGCM exhibits spectral scaling up to millennia in the North Atlantic in agreement with the reconstructed temperature variability in Greenland ice cores during the Holocene [Blender et al., 2006].

[5] MOC power spectra are generally assumed to follow a red-noise spectrum (Lorentzian),  $1/[f_0^2 + f^2]$ , with a damping time scale  $1/f_0$ , which was suggested by Hasselmann [1976] as a model for a damped, linear ocean forced by a white stochastic atmosphere. This cannot explain either long term memory or white high frequency response. Thus the aim of this work is to revisit the spectral behaviour of the MOC variability in the Atlantic on monthly to decadal time scales. Two 500 year control-runs with different state-of-the-art coupled AOGCMs (GFDL and ECHAM5/MPIOM) are analysed to investigate the main characteristics of the monthly MOC fluctuations. Emphasis lies on regime behaviour, scaling properties and possible long term memory. Both models and the detrended fluctuation analysis (DFA) are described in Section 2. Results for particular levels and latitudes are compared (Section 3). Section 4 follows with a discussion and conclusions.

### 2. Models and Analysis

[6] The Earth's climate is simulated by two coupled atmosphere-ocean general circulation models (AOGCMs), ECHAM5/MPIOM and GFDL. Both runs are pre-industrial control integrations prepared for the Intergovernmental

<sup>1</sup>Max-Planck-Institut für Meteorologie, Hamburg, Germany.

<sup>2</sup>Also at International Max-Planck Research School on Earth System Modelling, Hamburg, Germany.

<sup>3</sup>Meteorologisches Institut, Universität Hamburg, Hamburg, Germany.

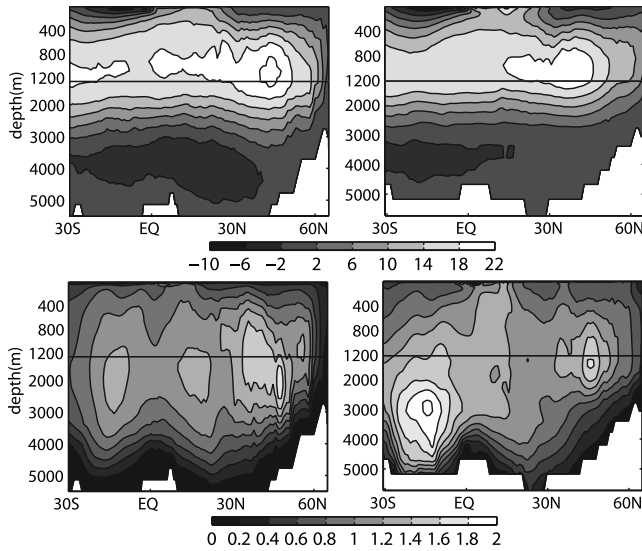


**Figure 1.** (top) Mean and (bottom) standard deviation of the zonally averaged stream function [Sv] in the Atlantic for (left) the GFDL model and (right) ECHAM5/MPIOM.

Panel on Climate Change (IPCC) Assessment Report AR4 simulations. The models do not employ flux adjustment.

### 2.1. ECHAM5/MPIOM and GFDL

[7] The coupled ECHAM5/MPIOM model consists of the atmospheric component ECHAM5 [Roegner *et al.*, 2003], which has a horizontal resolution of  $1.875^\circ \times 1.875^\circ$  (T63) and 31 levels. The ocean/sea ice component of the model, MPIOM [Marland *et al.*, 2004], has a  $1.5^\circ \times 1.5^\circ$  horizontal resolution on a curvilinear grid with 40 vertical levels. The grid poles are placed upon Antarctica and Greenland thus avoiding pole-singularity at the North Pole and providing high resolution (20–40 km) in the deep water formation regions of the Labrador Sea and the Greenland Sea. Various aspects of internal variability have been discussed by Jungclauss *et al.* [2006].

[8] The coupled GFDL model is run in the version CM2.1 [Delworth *et al.*, 2006] (data from: <http://nomads.gfdl.noaa.gov/CM2.X/CM2.1>). The atmosphere and land horizontal resolution is  $2^\circ \times 2^\circ$ ; the atmospheric model has 24 levels. The ocean resolution is  $1^\circ \times 1^\circ$ , with a meridional resolution equatorward of  $30^\circ$  becoming progressively finer, such that the meridional resolution is  $1/3^\circ$  at the equator. There are 50 vertical levels in the ocean, with 22 evenly spaced levels within the top 220 m. The ocean component has poles over North America and Eurasia to avoid polar filtering. Atmosphere and ocean are coupled through the Flexible Modeling System.

[9] Although these two integrations differ from each other in various aspects, the gross features of the Atlantic overturning are quite similar, i.e. northward inflow in the upper 1000–1500 m, the subsequent deep-water formation in the North Atlantic and southward spreading in the deep Atlantic, and Antarctic inflow from still deeper layers. The maximum meridional stream function is located around  $40^\circ\text{N}$ , between 1000 and 1500 m (Figure 1). The models tend to produce two regions of large standard deviation, one in the North Atlantic ( $45^\circ\text{N}$ , 1500 to 2000 m depth), and a

second one in the South Atlantic ( $20^\circ\text{S}$ , 1000 m to 4500 m), which is more intense in MPIOM.

### 2.2. Power Spectrum and Detrended Fluctuation Analysis

[10] Temporal variability of the MOC time series is analysed based on power spectra (determined using MATLAB, for 5 overlapping windows) and detrended fluctuation analysis (DFA). The DFA determines time scale dependent fluctuations in stationary anomaly sequences [Peng *et al.*, 1994]. The DFA is ideally suited to detect low frequency spectral power-law scaling in stationary time series if additional slow changes are present [Fraedrich and Blender, 2003; Blender and Fraedrich, 2003]. Thus the DFA is frequently superior to the power-spectrum in analysing geophysical time series. To support the results of the spectral analysis, the version DFA2 is applied, which eliminates possible long term trends caused by incomplete ocean spin-up integrations.

[11] For power-laws in the power-spectrum,  $S(f) \sim f^{-\beta}$ , the DFA fluctuation function scales as  $F(t) \sim t^\alpha$  with  $\beta = 2\alpha - 1$ . The autocorrelation function of the time series decays as  $C(t) \sim t^{-\gamma}$  with  $\alpha = 1 - \gamma/2$ . A time series has long term memory, if the integral of the autocorrelation function  $C(t)$  diverges. In this case  $\gamma < 1$  and the related exponents are  $\alpha > 1/2$  and  $\beta > 0$ . Stationarity of the time series is guaranteed for  $0 < \beta < 1$ . A stochastic process is denoted as white for  $\beta = 0$ , while  $\beta \approx 1$  is denoted as flicker or  $1/f$ -noise (acceptable for  $\beta$  from 0.7 to 1.3).

### 3. MOC Variability Regimes and Scaling

[12] The MOC is analysed in two levels, near 1200 m and 4000 m, and at the latitudes  $20^\circ\text{S}$ , EQ,  $20^\circ\text{N}$ ,  $40^\circ\text{N}$ , and  $60^\circ\text{N}$ , in both model runs. The upper level at 1200 m depth sits inside the MOC cell associated with the spreading of North Atlantic Deep Water whereas 4000 m depth sits inside the cell associated with the spreading of Antarctic Bottom

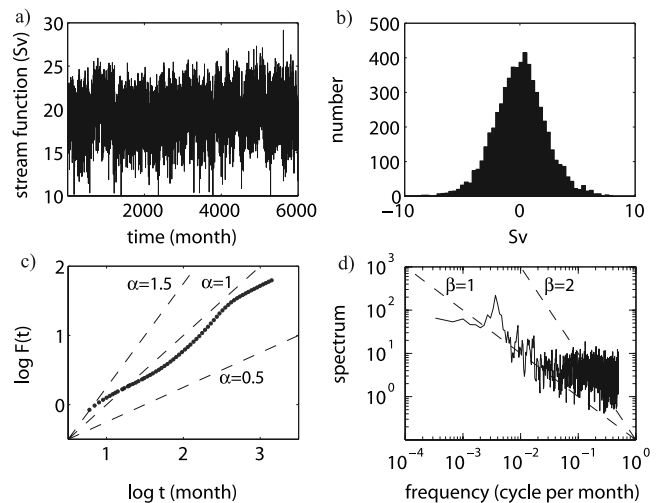


**Figure 2.** MOC at  $40^\circ\text{N}$  in 1200 m depth for the ECHAM5/MPIOM model: (a) time series, (b) anomaly frequency distribution, (c) fluctuation function by DFA2, (d) power-spectrum (5 overlapping windows). Dashed lines in Figures 2c and 2d denote power-laws for exponents  $\alpha$  and  $\beta$  as indicated.

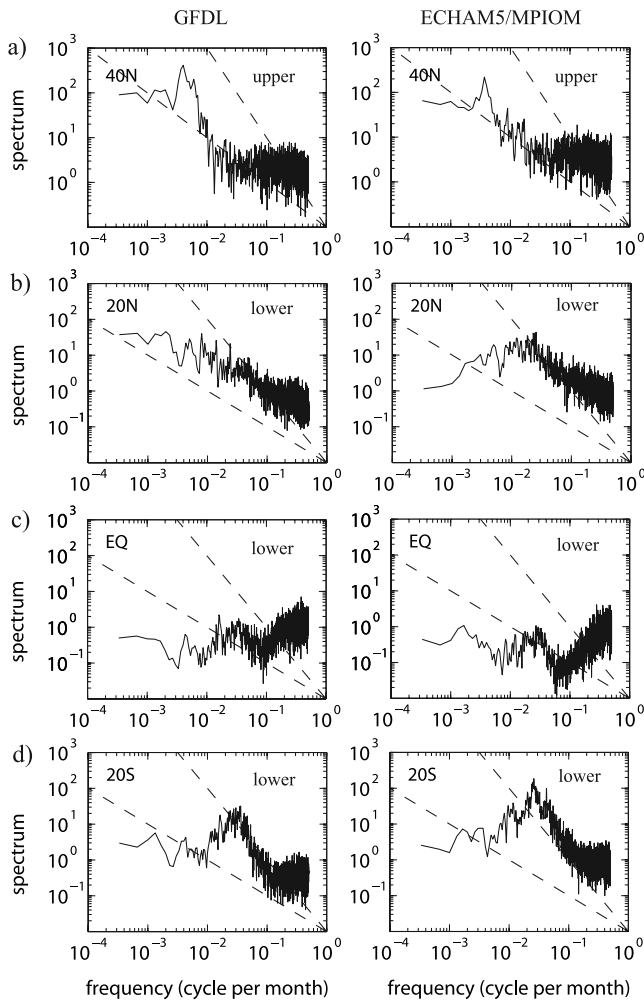


**Figure 3.** MOC Power spectra in (left) the GFDL and (right) ECHAM5/MPIOM model: (a) 40N upper ocean (near 1200 m), (b) 20N lower, (c) Equator lower, (d) 20S lower (lower ocean near 4000 m). Dashed lines indicate spectral exponents  $\beta = 1$  and  $2$ .

Water. Note that in ECHAM5/MPIOM (GFDL) there are 3 (4) model levels below 4000 m.

[13] In order to illustrate the main properties of the time series and to compare the power-spectrum with the DFA fluctuation function, the MOC at 40N and 1200 m depth from the ECHAM5/MPIOM model is chosen (Figure 2). The time series (a) shows that the MOC has become stationary; the remaining parts of this figure and the analyses are based on anomalies (annual cycle subtracted). Stationarity is checked for all time series (including lower levels) and the low frequency power spectra show no differences to the trend-eliminating DFA2. The frequency distribution (b) indicates that the MOC can be considered as Gaussian. The DFA fluctuation function (c) increases roughly according to  $F(t) \sim t^\alpha$ , with  $\alpha \approx 1$ . Three regimes can be identified with  $\alpha \approx 0.5$  for both short and long time scales, while  $\alpha \approx 1 \dots 1.5$  in an intermediate range. The exponents in the power-spectrum (d) are related by  $\beta = 2\alpha - 1$  and hint to  $\beta \approx 0$  and  $\beta \approx 1 \dots 2$  in the corresponding time scale ranges. The intermediate range

spectrum can either be interpreted as a Lorentzian (red-noise, with  $f^{-2}$ ), or as a reminiscent of  $1/f$  noise.

[14] In the upper ocean (near 1200 m depth) the following results are found (for brevity only the latitude 40N is presented in Figure 3). In the tropical Atlantic, 20S–20N, both models reveal a white noise spectrum (consistent with a DFA2 scaling  $\alpha \approx 0.5$ ), besides a peak with a period of 2 to 3 years. The white spectrum is even more pronounced in the equatorial region and 20N appears as a transition range. In the North Atlantic (Figure 3a), three frequency regimes appear: (i) For the highest frequencies (months to 3 years), white noise dominates in all upper level time series. (ii) In the transition range (3 to 30 years) a steep decay is determined with DFA scaling  $\alpha$  slightly above 1, different from red noise ( $\alpha = 1.5$ ). (iii) At periods of about 30 years an oscillation is superimposed [see *Eden and Greatbatch, 2003*]. (iv) For low frequencies (beyond 30 years) white background fluctuations occur. Besides the different intensities at 30 years, GFDL and ECHAM5/MPIOM give consistent results for MOC scaling in the upper ocean.

[15] In the deep ocean (near 4000 m depth) the spectral behaviour is less clear since the spectra differ largely for the different latitudes and the two models (Figure 3). The following results are noted: (i) The white noise plateau for high frequencies in the upper ocean is not observed at the lower depth. Instead, at the equator, power increases in the high frequency range, which is due to frictional damping of slower processes variability in the bottom levels (while intensities at highest frequencies remain unchanged). (ii) At 20N (b), both models behave differently for low frequencies; while the ECHAM5/MPIOM spectrum rises with increasing frequency the GFDL spectrum shows long term memory and  $1/f$  fluctuations throughout the accessible range of years to hundred years. (iii) At the equator (c), the spectrum increases for high frequencies (blue noise) and indicates white noise for low frequencies, similar in both models. (iv) In the South Atlantic (d, 20S), an oscillation with 3 years period is superimposed on the white background noise. (v) At 40N the 30 year oscillations extends to the deep ocean in the GFDL model.

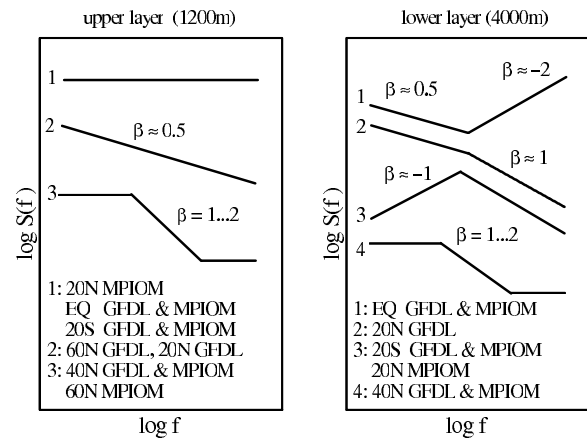


**Figure 4.** Sketch of main types of MOC power spectra found in the upper and lower level with ranges for the spectral exponent  $\beta$ . Locations of model spectra are indicated (see Figure 3).



#### 4. Summary and Discussion

[16] Regime behaviour of the variability of the Atlantic MOC is analysed in two state-of-the-art coupled atmosphere-ocean general circulation models, GFDL and ECHAM5/MPIOM, which are used for IPCC simulations. The simulations are designed as present-day control runs with durations of 500 years for which oceanic spin-up can be neglected. The variability of the monthly data is determined by power-spectra, which are supported by detrended fluctuation analysis (DFA version 2, which eliminates superimposed trends). The central aims of the analysis is the scaling properties of the spectra.

[17] The main result is the existence of regimes of variability with distinct power-law relationships in the spectra (see the sketch in Figure 4) demonstrating a general agreement between the two models. At high frequency, the spectrum in the upper ocean is white, which is very different from the Hasselmann [1976] model. This is because, at short time scales, the MOC reflects the projection in the vertical plane (after zonal averaging) of the topographic Sverdrup response of the ocean to the wind forcing, which determines its white spectrum and the characteristic barotropic structure at high frequencies (seen from high pass filtered MOC, with 3 years cut-off, not shown). The reason why this does not occur in the lower depth is due to the frictional damping in the bottom levels.

[18] The most frequent spectral power-law,  $S(f) \sim f^{-\beta}$ , is found for  $\beta \approx 1$ , which is denoted as  $1/f$  or flicker noise. Although red-noise ( $1/[f_0^2 + f^2]$ ) is one of the most frequently used type of power-spectrum, this functional relationship appears to be more an exception than the rule. These types are hints to conceptual theories of the underlying mechanisms of MOC variability (see Fraedrich et al. [2004] for a stochastically forced vertical diffusion model and for references to other models). In the North Atlantic an oscillation of about 30 years is found, while in the South Atlantic 2 to 3 years periodicity dominates, whose origin is still uncertain. While the majority of the spectra is consistent for the two models, discrepancies are found in the North Atlantic, mainly at lower depth.

[19] The absence of the red-noise spectra has consequences for frequently applied significance tests. In some spectra increasing variability for lower frequencies described by exponents  $\beta > 0$  is found. This indicates that the North Atlantic circulation possesses long term memory with consequences for the analysis of long term climate variability, trends, and the assessment of anthropogenic climate signals.

[20] **Acknowledgments.** We appreciate helpful comments of the reviewers and discussions with J. Jungclauss, J.-S. von Storch, R. Käse, J. Marotzke, and D. Stammer (Hamburg). We acknowledge support by Deutsche Forschungsgemeinschaft (SFB 512) and thank GFDL for data available at <http://nomads.gfdl.noaa.gov/CM2.X/CM2.1>. X. Z. received a Max Planck Institute for Meteorology stipend.

#### References

- Blender, R., and K. Fraedrich (2003), Long time memory in global warming simulations, *Geophys. Res. Lett.*, *30*(14), 1769, doi:10.1029/2003GL017666.
- Blender, R., K. Fraedrich, and B. Hunt (2006), Millennial climate variability: Simulation and Greenland ice cores, *Geophys. Res. Lett.*, *33*, L04710, doi:10.1029/2005GL024919.
- Delworth, T. L., and R. J. Greatbatch (2000), Multidecadal thermohaline circulation variability driven by atmospheric surface flux forcing, *J. Clim.*, *13*, 1481–1495.
- Delworth, T. L., A. J. Broccoli, A. Rosati, R. J. Stouffer, V. Balaji, J. A. Beesley, W. F. Cooke, K. W. Dixon, J. Dunne, and K. A. Dunne (2006), GFDL's CM2 global coupled climate models: Part I. Formulation and simulation characteristics, *J. Clim.*, *19*, 643–674.
- Eden, C., and R. Greatbatch (2003), A damped decadal oscillation in the North Atlantic climate system, *J. Clim.*, *16*, 4043–4060.
- Eden, C., and T. Jung (2001), North Atlantic interdecadal variability: Oceanic response to the North Atlantic Oscillation (1865–1997), *J. Clim.*, *14*, 676–691.
- Eden, C., and J. Willebrand (2001), Mechanisms of interannual to decadal variability of the North Atlantic circulation, *J. Clim.*, *14*, 2266–2280.
- Eden, C., R. J. Greatbatch, and J. Lu (2002), Prospects for decadal prediction of the North Atlantic Oscillation (NAO), *Geophys. Res. Lett.*, *29*(10), 1466, doi:10.1029/2001GL014069.
- Fraedrich, K., and R. Blender (2003), Scaling of atmosphere and ocean temperature correlations in observations and climate models, *Phys. Rev. Lett.*, *90*, 108501, doi:10.1103/PhysRevLett.90.108501.
- Fraedrich, K., U. Luksch, and R. Blender (2004),  $1/f$ -model for long time memory of the ocean surface temperature, *Phys. Rev. E*, *70*, 037301, doi:10.1103/PhysRevE.70.037301.
- Frankignoul, C., P. Müller, and E. Zorita (1997), A simple model of the decadal response of the ocean to stochastic wind stress forcing, *J. Phys. Oceanogr.*, *27*, 1533–1546.
- Hasselmann, K. (1976), Stochastic climate models: Part I. Theory, *Tellus*, *28*, 473–484.
- Huybers, P., and W. Curry (2006), Links between annual, Milankovitch and continuum temperature variability, *Nature*, *444*, 329–332.
- Jayne, S. R., and J. Marotzke (2001), The dynamics of wind-induced ocean heat transport, *Rev. Geophys.*, *39*, 385–411.
- Jungclauss, J., M. Botzet, H. Haak, N. Keenlyside, J.-J. Luo, M. Latif, J. Marotzke, U. Mikolajewicz, and E. Roeckner (2006), Ocean circulation and tropical variability in the AOGCM ECHAM5/MPI-OM, *J. Clim.*, in press.
- Junge, M., and K. Fraedrich (2006), Temperature anomalies in the northeastern North Atlantic: Subpolar and subtropical precursors on multiannual time scales, *Journal of Climate*, in press.
- Marsland, S. J., N. L. Bindoff, G. D. Williams, and W. F. Budd (2004), Modelling water mass formation in the Mertz Glacier Polynya and Adelie Depression, East Antarctic, *J. Geophys. Res.*, *109*, C11003, doi:10.1029/2004JC002441.
- Peng, C.-K., S. V. Buldyrev, S. Havlin, M. Simons, H. E. Stanley, and A. L. Goldberger (1994), On the mosaic organization of DNA sequences, *Phys. Rev. E*, *49*, 1685–1689.
- Roeckner, E., et al. (2003), The atmospheric general circulation model ECHAM5: Part I. Model description, *Rep. 349*, 127 pp., Max-Planck-Inst. für Meteorol., Hamburg, Germany.
- Sturges, W., and B. G. Hong (1995), Wind forcing of the Atlantic thermocline along 32°N at low frequencies, *J. Phys. Oceanogr.*, *25*, 1706–1715.
- von Storch, J.-S., P. Müller, R. J. Stouffer, R. Voss, and S. F. B. Tett (2000), Variability of deep-ocean mass transport: Spectral shapes and spatial scales, *J. Clim.*, *13*, 1916–1935.
- Willebrand, J. S., S. G. H. Philander, and R. C. Pacanowski (1980), The oceanic response to large-scale atmospheric disturbances, *J. Phys. Oceanogr.*, *10*, 411–429.
- R. Blender and K. Fraedrich, Meteorologisches Institut, Universität Hamburg, Bundesstrasse 55, D-20146 Hamburg, Germany. (klaus.fraedrich@zmaw.de)
- X. Zhu, Max-Planck Institut für Meteorologie, Bundesstrasse 53, D-20146 Hamburg, Germany.